Available online at https://asric.africa/natural-sciences
ASRIC Journal on Natural Sciences Vol 3(1) (2023) 220-236

Identification of high Groundwater Potential Locations in the Atebubu Municipality of Ghana using the Electrical Resistivity Method

Alfred K. Bienibuor[1]*, Kwasi Preko[2], Akwasi A. Aning[2] Aboagye Menyeh[2], David D. Wemegah[2]

[1]Department of Chemical Sciences, University of Energy and Natural Resources, P. O. Box 214, Sunyani, Ghana

[2]Department of Physics, Geophysics Section, Kwame Nkrumah University of Science and Technology, Kumasi, Ghana

*Corresponding author: alfred.bienibuor@uenr.edu.gh

Abstract

The Atebubu municipality has been battling with a perennial potable water crisis for the past few decades. Borehole and well contractors in the municipality have been using nonscientific means to site aquifers prior to drilling, and this is the major cause of the high incidence of dry boreholes often recorded. Most of the hand-dug wells and boreholes are only productive during the raining season. This problem affects economic activities, children's education and the quality of life of the people. This paper used the electrical resistivity method in the Wenner and gradient array configurations to access subsurface groundwater information leading to high yielding groundwater potential locations. The results show resistivity values for both Wenner and gradient techniques ranging from 5 to 2212 Ωm across the profiles. Resistivity distributions in the very low bracket, interpreted as clay contents, ranged from 5 to 210 Ωm and dominate the shallow subsurface to about 50 m. The thickness of this layer is approximated at 10 to 20 m. Moderately low resistivity distributions (from 100 to 506 Ωm) were observed at deeper depth with only few portions stretching to the middle belt. This bracket of the resistivity distribution is interpreted as water contents, while the high to very high values which are interpreted as competent rock formations were observed predominantly at both deeper depth and the middle belt. High yielding aquifers are therefore expected to be intercepted at deeper depths, overlain at most locations by a clayey vadose zone. Though results of the two measurement techniques significantly corroborated, the Wenner technique appears to suggest that more than half of the depth probed could be clay content, opposed to the gradient technique which portrays more fractured rocks, revealing better chances of high yielding groundwater potential at the sites identified.

Keywords: Atebubu, yielding, groundwater, borehole, surface water

1. Introduction

Groundwater refers to the water in cracks and spaces of rocks, gravels and soils in the saturated zone beneath the Earth surface (Figure 1). It is essential for socioeconomic development in every facet of life. Many people across the globe are now turning to groundwater as the safest and best reliable option for their major source of water (Bienibuor et al., 2020; Taylor et al., 2013; Margat and Van der Gun, 2013, Hakim et al, 2009), resulting in the water withdrawal outweighing annual replenishment (Saha et al., 2018). Coupled with the vulnerability of groundwater to pollution from both geogenic and anthropogenic sources

(Agyare et al., 2021; Saha et al., 2018), there is the need for pragmatic measures to ensure continuous supply and quality.

One major problem of groundwater harvesting is siting the appropriate aquifer for drilling. Confined aquifers might suffer vertical recharging, though the confining layer could serve as a protective cover from anthropogenic pollution sources (Ho and Sa, 2014). Unconfined aquifers on the other hand have the advantage of getting recharged by surface runoffs from rainfall, snow melt, etc., but are also more vulnerable to anthropogenic pollutants (Almanza Tovar et al., 2020; Yesilnacar and Sahinkaya, 2012). Fortunately, geophysical methods are able to locate and identify the type of aquifer, even at deeper depths (Bienibuor et al., 2016; Aning et al., 2014; Andrews et al., 2013). Hence, to drill high-yielding and sustainable boreholes, geophysical techniques must be employed in siting the appropriate aquifer, its depth and delineating the vadose characteristics before drilling.

The sustainability of boreholes and hand-dug wells usually depends on the nature of the vadose zone, drilling depth and type of aquifer (Li et al., 2017; Cao et al., 2016). The nature of the vadose zone can either enhance or inhibit aquifer recharge. For instance, a clay, mudstone or shale-dominated vadose zone will definitely affect the ease with which water percolates through it to recharge the aquifer beneath it (Acharya et al., 2017; Fynn et al., 2016). Aside that, the vadose zone also contributes to determining the type of aquifer (confined, unconfined, semi-confined or perched). In addition, boreholes drilled to deeper depths are less prone to anthropogenic pollution sources as opposed to that drilled to shallower depths (Egbueri and Mgbenu, 2020; Ho and Sa, 2014; Essien and Bassey, 2012). The migration of groundwater to recharge aquifers, both vertically and horizontally, is influenced by hydraulic conditions (Osei et al., 2017; Zhu et al., 2015; Preko et al., 2009; Smerdon et al., 2008; Gemitzi et al., 2006).

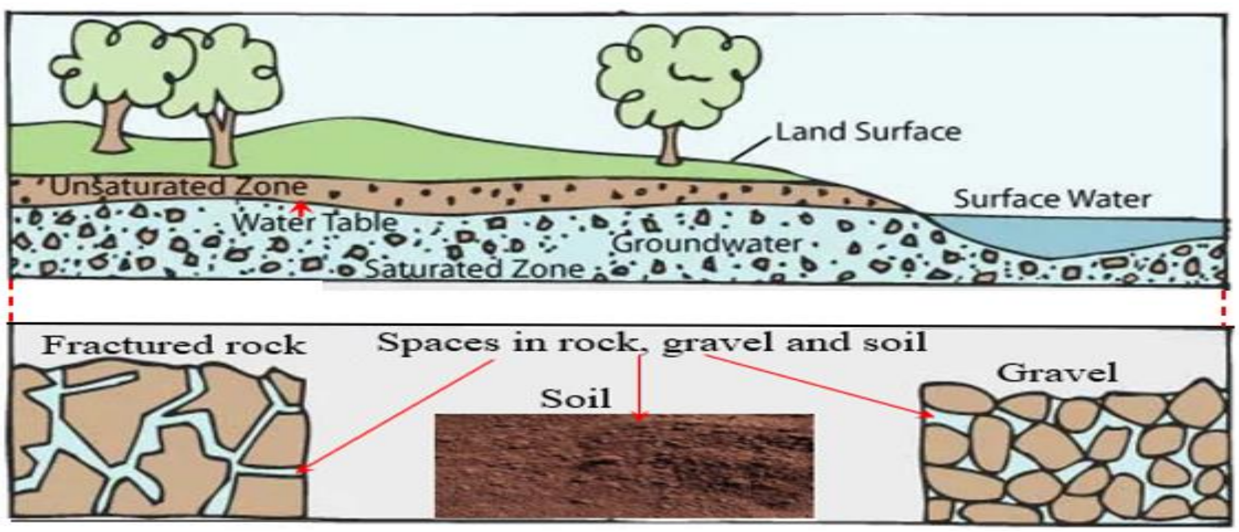

Figure 1: Illustration of Groundwater occurrence (modified after Afrose et al., 2018)

Vertical recharge, resulting from runoffs and surface water bodies is directly and more affected by precipitation temperature and evapotranspiration (Sasidharan et al., 2020; Haidu and Nistor, 2020) than horizontal recharges from migrating waters from saturated soils, adjourning aquifers and other surface waters (Alazard et al., 2016; Praamsma et al., 2009). In the same way, hydraulic pressure varies from aquifer to aquifer even at different locations of the same aquifer (Ghazavi et al., 2018; Zhang et al., 2019). At a given depth, the absolute hydraulic pressure (P_{abs}) is equal to the sum of the hydrostatic pressure (P_w) and the atmospheric pressure (P_{atm}):

$$P_{abs} = P_{atm} + P_w$$

The hydrostatic pressure (resulting from the water alone), P_w depends on the height h of the water in the aquifer (or the thickness of the saturation of the aquifer), the density of water, ρ and gravity, g:

$$P_w = \rho gh$$

The atmospheric pressure influence, on the other hand, depends on the aquifer type. For confined aquifers, atmospheric pressure is less than the pressure on the aquifer. Shahbazi et al. (2020) and Hristopulos (2003) reported that the properties of subsurface geological materials substantially influence the isotropy and homogeneity of hydraulic conductivity of the subsurface. For an isotropic geological formation, hydraulic conductivity does not depend on the direction of measurement nor on position for a homogeneous formation (Shahbazi et al., 2020; Stober and Bucher, 2015). The formation is heterogenous if hydraulic conductivity varies from place to place (Maxwell and Kollet, 2008).

Land use and land cover also have significant impacts on groundwater recharge and discharge rates (Nepf et al., 2022; Yifru et al., 2021; Tahiru et al., 2020; Zomlot et al., 2017; Gebere et al., 2016; Owuor et al., 2016; Scanlon et al., 2005). Using the Soil Water Assessment Tool (SWAT) and the Newton Modular Finite Difference Groundwater Flow (MODFLOW-NWT) in their study, Yifru et al. (2021) realised that vegetative land covers had higher infiltration rates than impervious covers. The vegetation, through the growth of its roots, creates more pores in the soil, and this introduces soil organisms like worms, termites, millipedes, mites, etc., into the soil, further aerating the soil (Nepf, et al., 2022; Ghestem et al., 2011). Hence, forested lands have higher infiltration rates than all other vegetative types (Ghestem et al., 2011). Impervious surfaces like roads, parking lots, etc., on the other hand, inhibit infiltration (Naeem et al., 2021) and, therefore, retards groundwater recharge. The worsening water crisis in Atebubu may be linked, in part, to the speedy development of the area. Urbanisation converts vegetative land covers to impervious ones through the construction of roads, houses, parking lots, etc., which impedes groundwater recharge (Manley et al., 2022; Togbévi et al., 2022; Naeem et al., 2021; Wakode et al., 2018; Carlson et al., 2011; Sharp, 2010; Naik et al., 2008).

2. Methodology

2.1 Project Site Description

The study was conducted in Atebubu, the capital city of the Atebubu-Amanten Municipality. Atebubu is situated between latitudes 7° 23' N and 8° 22' N and longitudes 0° 30' W and 1° 26' W in the Atebubu-Amanten Municipality, Bono East Region. The main economic activity in the area is farming, with yam being the dominant crop. The municipality falls within the southern part of the Voltaian supergroup, with undifferentiated rocks of the Oti-Pendjari and the Obosum groups (Figure 2; Entsua-Mensah et al., 2007). These groups consist of sandstone, shale, mudstone, limestone, sandy and pebbly beds (Asare-Donkor and Adimado, 2020; Hadzi et al., 2019; Agyekum and Asare, 2016; Yidana et al., 2014; Forkuor et al., 2013; Agyekum et al., 2013; Akayuli et al., 2013).

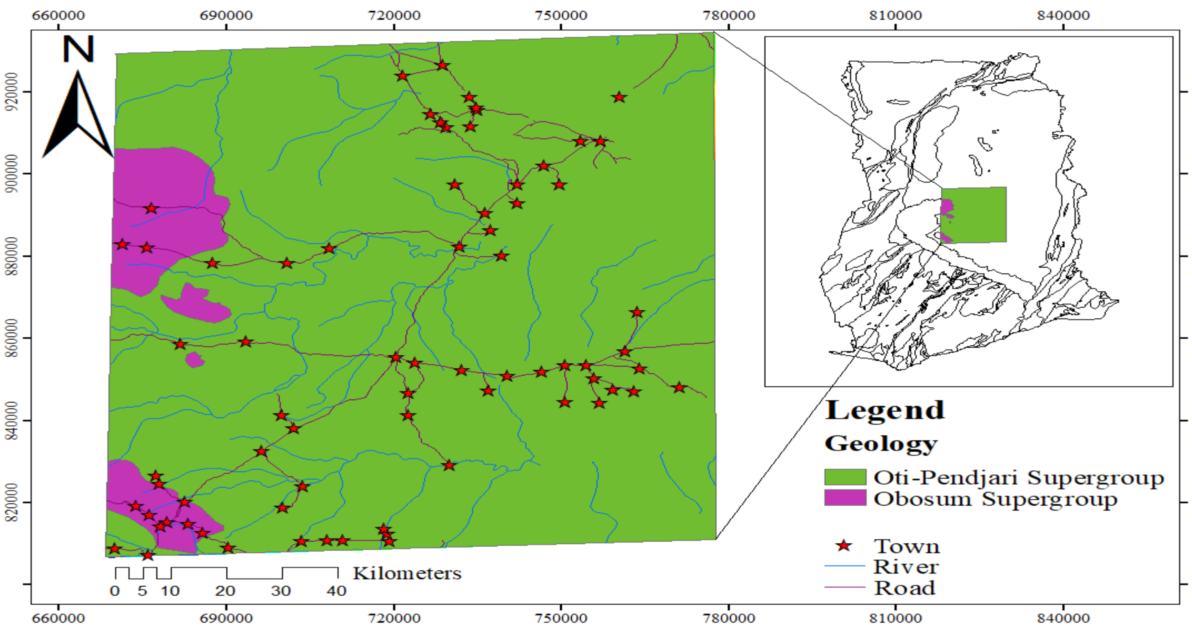

Figure 2: Geological map of the study area

Groundwater potential in the Voltaian Supergroup is the lowest among the hydrogeological provinces of Ghana (Appiah-Adjei and Osei-Nuamah, 2017; Banoeng-Yakubu et al., 2011) with an average borehole yield range of 6.2 to 8.5 m^3/h (Mainoo et al., 2019; Gyau-Boakye and Dapaah-Siakwan, 2000). The primary porosity and permeability of rocks are negligibly small and, therefore, they are not favourable for groundwater development. The low primary porosity is due to the imperviousness of the rocks of the formation (Mainoo et al., 2019; Yidana et al., 2008). Secondary porosity largely controls fracture and faulting in the rocks (Sunkari et al., 2021; Chegbeleh et al., 2020; Yidana et al., 2019). Success rate of boreholes in the formation is as low as 56 % (Yidana et al., 2019; Yidana et al., 2010; Dapaah-Siakwan and Gyau-Boakye, 2000), and the few productive ones are low yielding.

2.2 Data Acquisition

The resistivity data was acquired by the ABEM terrameter SAS4000 C in both Wenner and gradient electrode configurations. Figure 3 is a map showing the profiles along which data was taken. The total length of profiles was 400 m.

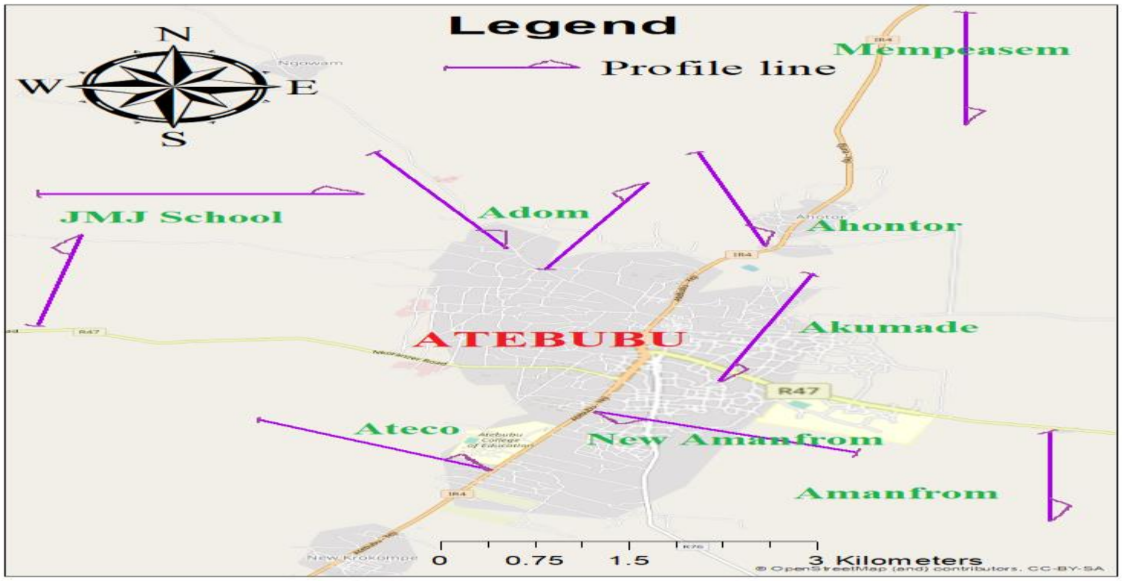

Figure 3: Layout of the study area, showing profile lines.

One profile each was probed at Akumade, New Amanfrom, Amanfrom, Ahontor, Mempeasem and Atebubu College of Education communities, trending in different directions. Position coordinates and elevations of profiles probed are indicated on table 1. At Adom two profiles were surveyed. Profiles 1 and 2 trended north east and south east respectively. Two profiles were also constructed at the JMJ School premises. Profile 1 was constructed to trend in the north eastern direction while profile 2 was constructed from west to east. Each profile accommodated forty-one (41) electrodes, laid at 10 m spacing.

Though the terrameter equipment has been used successfully for geophysical investigations in various places (Hussain et al., 2020; Martínez et al., 2019; Arifin et al., 2019; Nero et al., 2016; Pellicer and Gibson, 2011), there is no literature on its suitability for use in the Atebubu-Amanten Municipality. The electrode test was done before measurement commenced. On the field, it did not encounter any significant problems. There were a few times measurements were interrupted due to overheating of the equipment or related issues. On the part of overheating, iced blocks were wrapped around it to aid cooling, and this helped the survey. For interruptions due to other minor issues, the equipment was merely restarted. In very rare instances, some electrodes were skipped for measurements to continue.

Table 1: Position coordinates and elevations of profiles probed

Community	Profile	Position	Latitudes [ºN]	Longitudes [ºW]	Elevation [m]
New Amanfrom	1	Starting	7º43' 58.764''	0º59' 18.282''	137.30
		Middle	7º44' 1.674''	0º59' 23.91''	142.10
		Ending	7º44' 4.368''	0º59' 29.922''	141.90
Atebubu College of Education	1	Starting	7º43' 43.872''	0º59' 51.564''	142.20
		Middle	7º43' 46.608''	0º59' 57.096''	144.40
		Ending	7º43' 50.526''	1º0' 2.856''	127.80
Ahontor	1	Starting	7º46' 42.81''	0º58' 36.258''	130.00
		Middle	7º46' 37.14''	0º58' 33.498''	144.40
		Ending	7º46' 30.816''	0º58' 31.182''	107.50
Mempeasem	1	Starting	7º47' 30.51''	0º58' 21.21''	131.90
		Middle	7º47' 24.048''	0º58' 20.34''	133.20
		Ending	7º47' 17.838''	0º58' 19.362''	131.90
Akumade	1	Starting	7º44' 51.534''	0º59' 13.962''	133.80
		Middle	7º44' 45.45''	0º59' 16.398''	124.80
		Ending	7º44' 39.414''	0º59' 19.146''	128.60
JMJ	1	Starting	7º44' 57.276''	1º00' 4.584''	175.40
		Middle	7º45' 3.774''	1º00' 3.108''	177.70
		Ending	7º45' 10.056''	1º00' 0.438''	177.90
	2	Starting	7º44' 53.184''	0º59' 59.142''	87.60
		Middle	7º44' 53.01''	0º59' 53.166''	141.30
		Ending	7º44' 52.524''	0º59' 45.972''	155.20
Amanfrom	1	Starting	7º43' 32.688''	0º59' 10.962''	197.50
		Middle	7º43' 25.5''	0º59' 10.722''	148.30
		Ending	7º43' 18.54''	0º59' 10.266''	178.70
Adom	1	Starting	7º46' 9.234''	0º59' 31.89''	139.50
		Middle	7º46' 3.552''	0º59' 34.56''	138.20
		Ending	7º45' 57.822''	0º59' 37.782''	125.30
	2	Starting	7º46' 34.092''	0º59' 58.494''	142.80
		Middle	7º46' 28.212''	0º59' 55.524''	144.50
		Ending	7º46' 22.572''	0º59' 52.488''	127.10

2.3 Data processing and interpretation

Data was processed using the RES2DINVx64 software, a computer program which automatically determines a 2D resistivity model of the subsurface from the field data. The program supports multicore central processing units (CPUs). Inversion is simply dividing the data into rectangular blocks which represent the distribution of the data. The depths of these blocks equal the depths of investigation. In this paper the data was read into the software and edited for electrode positions, discretisation, etc. before modelling. For the model discretisation, extended model was set to 'No', so that trapezoid models are obtained instead of rectangular models. At model display in the show inversion results section, the resistivity option was chosen to display it. Results were displayed after six iterations. Bad data points, referred to as data outliers (Figure 4) were then statistically removed using the RMS error statistics analysis. Data outliers are data misfits between measured and calculated apparent resistivity values. These may result from poor electrode contact with the ground due to indurated surficial materials or dry ground, shorting due to very wet ground conditions and relay failures at some electrodes.

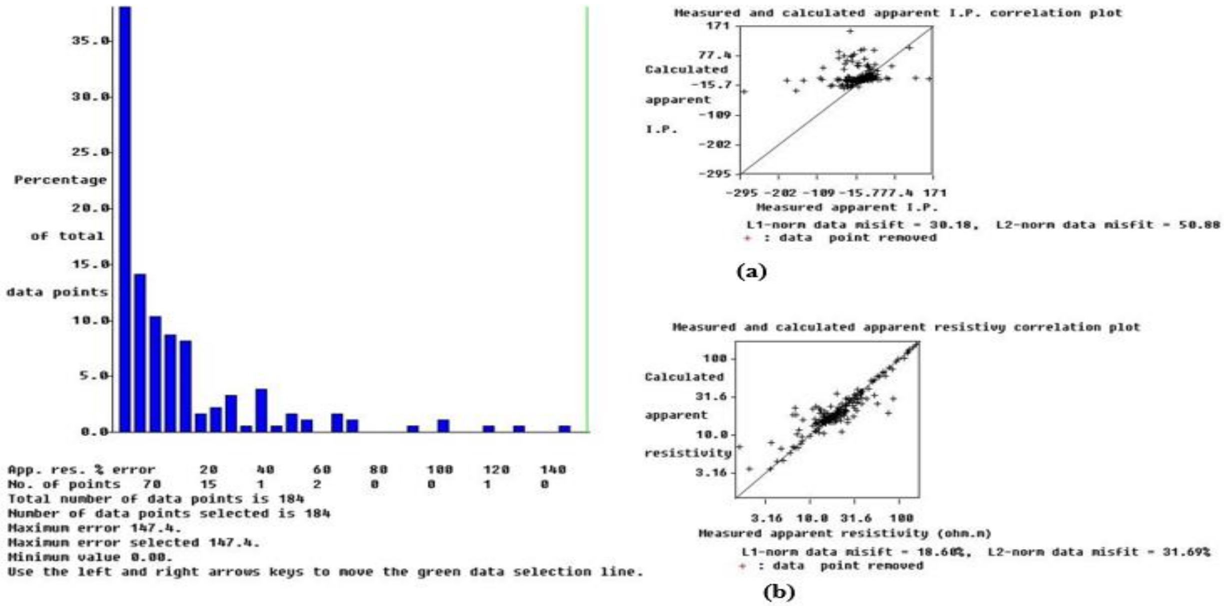

Figure 4: Histogram and scatter plots for inversion results, showing data outliers.

The filtered data was saved with a new filename, reread into the software and the inversion process was repeated. The entire process was repeated until less RMS error was obtained (preferably less than 10 %). The final models were then saved.

3. Error analysis

In designing a survey or processing geophysical data, it is imperative to consider all sources of error to have an idea of possible artefacts or inaccuracies in your models. In resistivity surveys, it is possible to remove noisy data prior to inversion and modelling (Miller et al., 2008). In this work, the RMS error statistical analysis was used to remove noisy data and artefacts before Processing to improve the resolution and quality of models. The inversion was done with high RMS until the lowest possible absolute errors were achieved, since absolute error assesses the signal-to-noise ratio of a dataset. According to Rucker et al. (2011), absolute error refers to the absolute difference of two repeated readings. In this survey only few extremely noisy data were recorded, where the absolute errors equaled or exceeded 10. This was quite expected since resistivity measurements are usually less prone to noise (Mashhadi and Ramazi, 2018; Dahlin et al., 2002).

Major sources of systematic and random errors were the aging of cables, wires or electrodes and impedance effects (Mashhadi et al., 2020; Dahlin et al., 2002). The non-ideal nature of the terrameter system could also introduce systematic errors. Another key source of error was the electrode spacing. Electrode spacing errors are errors associated with electrode position measurements or inadvertent electrodes on the. Most of the profiles were constructed on bushy sites. Coupled with the undulating and rough ground surfaces, it was challenging to have straightened cables along the profiles. Additionally, indurated surficial materials or dry ground can cause poor electrode contact with the ground, shorting due to very wet ground conditions and relay failures at some electrodes resulted in shifting some electrode positions, potentially affecting their spacing. To minimize minimise electrode spacing errors on the field, the data acquisition team ensured maximum care and vigilance throughout the exercise, particularly during the mounting of electrodes. Two technicians were assigned to check and ensure correct electrode positions before measurements on each profile commenced. Additionally, a reconnaissance survey was conducted to assess the potency of the equipment and electrode configuration techniques in order to minimise observed potential and related errors. Furthermore, the survey was repeated two to three times before the results were stored in communities with background noise such as passing vehicles.

4. Results and Discussion

The 2D data was inverted into resistivity models, showing both lateral and vertical subsurface resistivity distribution. The models revealed a wide variation of subsurface information. These model sections were displayed using user defined logarithmic contours. Information on these models reveal the nature and type of subsurface materials. The study area is characterized by high clay content (Sowley and Aboagye, 2010; Abonkrah, 2004), therefore the resistivity of the subsurface could be evidence of the presence of either clay or water contents. However, since clay is more conductive than water (Mainoo et al., 2019; Madun et al., 2018; Saad et al., 2012; Ewusi et al., 2009), very low resistivity layers, indicated in this case as blue, are interpreted as clay contents while layers of moderately low resistivity values, indicated by the green contours could be the aquifer zones. The thickness of clay content is approximated at 10 to 20 m.

In both gradient and Wenner techniques the results indicate a wide variation of subsurface resistivity distributions, ranging from 5 to 2818 Ωm across the profiles. Values of resistivity in the very low bracket for all the models ranged from 5 to 98.6 Ωm while the moderately low resistivity bracket, purported to be water contents, have values ranging from 100 to 500 Ωm. The very low resistivity values were observed over the shallow subsurface, covering about one-third of the vadose zone. Fractured rocks of the moderately low resistivity values were observed over the basement rocks. In all the profiles, results for both the gradient and Wenner configurations show great signs of competent aquifers at deeper depths, though they poorly correlate for most of the profiles.

Very low resistivity values were observed across most of the top layers with the moderately low values characterising the middle belt. The green contours marked A at Akumade and Amanfrom (Figure 5) could be highly fractured rocks with high water contents since resistivity values of these enclaves are in the range of 100 to 500 Ωm, which are within values observed by Razak and Muztaza. (2022), Azizan et al. (2018) and Juanah et al. (2013), as high groundwater potential. Both results show great signs of high yielding groundwater potentials of the basement rocks with rocky first layers and thick clayey middle layers. Structures are however better resolved for Amanfrom than Akumade as results of the gradient and Wenner measurements were significantly compared for Amanfrom than for Akumade. Recommended drilling points, indicated by the red arrows, are points 230 and 90 m for Akumade and 190 m for Amanfrom.

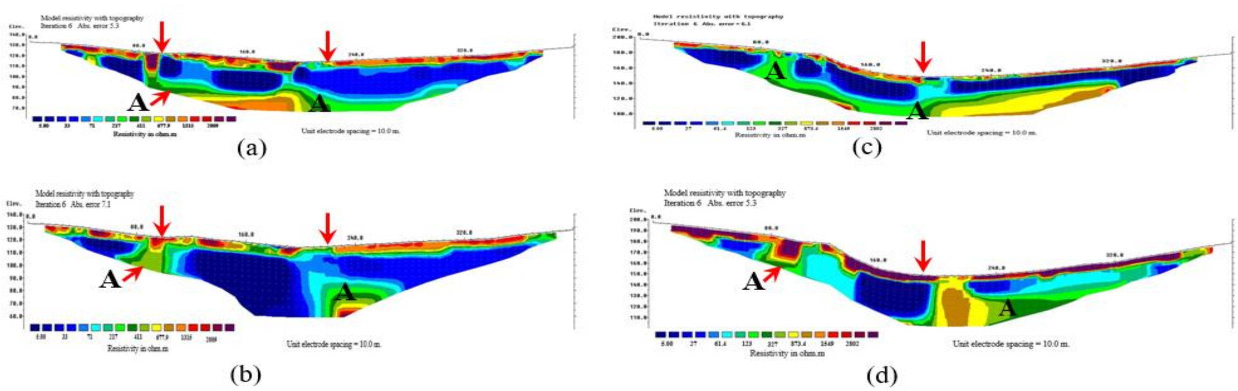

Figure 5: The diagram represents gradient and Wenner resistivity models, (a) and (b) for Akumade and (c) and (d) for Amanfrom communities respectively.

At the Adom community two profiles (1 and 2) were surveyed, trending north east and south east respectively. Results of the two measurement techniques corroborated more significantly for profile 2 than for profile 1. In the case of profile 1, about 90 % of the depth probed, from about 110 to 205 m, is revealed by the Wenner technique as clay contents which is at variance with the competent basement rock recorded in the same region by the gradient measurement (Figures 6 a & b). The green contoured layers are also better interconnected for the gradient technique than the Wenner, which is an indication of better groundwater prospects with the gradient method than with the Wenner method. Also, though the contours labelled A on profile 1 appear to match for the two measurement techniques, a highly resistive layer is observed beneath that for the Wenner results. Results of profile 2 on the other hand reveals a highly resistive shallow subsurface as observed on both models (Figures 6 c & d), a possible hard rock layer, with indications of fractured basement rocks. The competent rock condition and clayey block expressed at the bottom layer and middle belt are also well corroborated for both gradient and Wenner results. The green contours are also well interconnected, suggestive of high water contents. Recommended drilling points for profiles 1 and 2 are 215 and 210 m respectively.

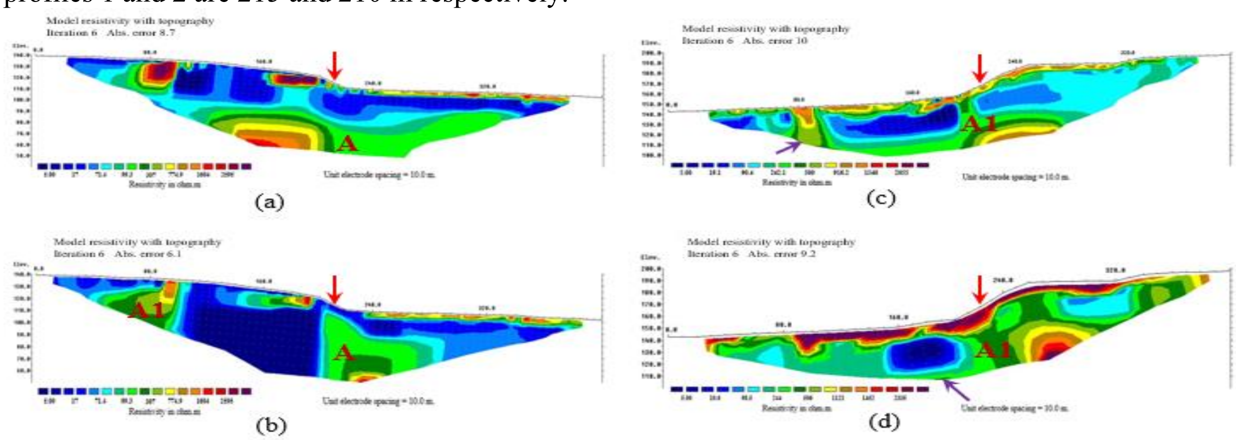

Figure 6: Gradient and Wenner resistivity models for Adom community: (a) and (b) for profile 1 and (c) and (d) for profile 2 respectively.

At the JMJ community the topography of profile 1 was fairly flat, but quite steep for profile 2. On both profiles the gradient array results indicate that more than half of the eastern part of the profile is characterised by crystalline rocks over the middle belt, stretching to greater depths. This is corroborated by the Wenner array results of profile 2. Expressions of hard rock conditions were observed at the basement of profile 1 with the Wenner array measurement between 180 and 250 m. A lot of data was lost at the extreme ends of the south western and south eastern belts with the Wenner array measurements; nevertheless, structures resolved were matched with that of the gradient array measurements. The fracture or fault zone for profile 1 is identified with resistivity values ranging from 201 to 342 Ωm and 200 to 437 Ωm for profile 2, indicated by the green contours. Drilling at points 110 m and 195 m on profile 1 (Figures 7 a & b) is expected to intercept the fractured rocks at these contour locations. Point 195 m however is more preferred to point 110 m. For profile 2 recommended drilling points are points 90 and 260 m (Figures 7 c & d). Though the Wenner array results predicts a hard, unfractured rock layer beneath point 260 m, it is still recommended because contour I could extend both eastwards and westward as the profile was constructed from west to east.

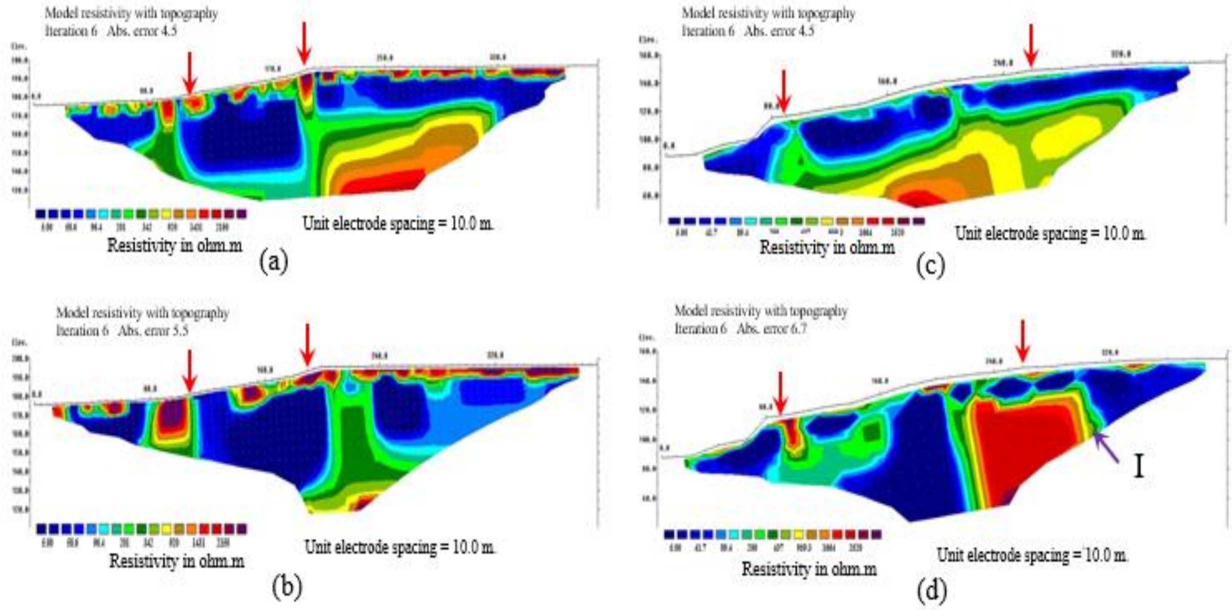

Figure 7: Gradient and Wenner resistivity models for JMJ School community: (a) and (b) for profile 1 and (c) and (d) for profile 2 respectively.

Diverse resistivity distributions were observed at the Ahontor and Mempeasem communities with values of the fault zone from 238 to 500 Ωm for Ahontor and 159 to 309 Ωm for Mempeasem. At Ahontor structures revealed with the gradient method do not sufficiently conform to that by the Wenner technique. With the gradient method results, the first layer is expected to comprise of hard, unfractured rocks, up to a few meters. This is then followed by a possible thick clay layer characterising the entire middle belt and the extreme ends of the profile. On the Wenner method model on the other hand, expressions of hard rock conditions were noticed on the first layer and stretches to the middle belt at points 90 to 110 m and 200 to 215 m locations. Nevertheless, the green contours on both models are well aligned at points 115 and 265 m as indicated by the red arrows (Figures 8 a & b). Also, the yellow contour (E) at the basement from points 105 to 255 m on the gradient model conforms to contour E on the Wenner model. The two blocks are expressions of a competent rock. At Mempeasem a highly resistive layer, suggestive of a massive rock was observed stretching from the middle belt to the far depth of about the 70 to 320 m location on the profile as shown by the yellow to red layers of contours (Figures 8 c). This massive bedrock expression on the gradient model is well corroborated by the Wenner method results as the highly resistive blocks, C and D dip towards each other, a sign that they could extend to intercept at depth. The top layers however, are mismatched. The gradient results portray a clay dominated top layer while the Wenner results reveals a fractured one. Groundwater potential on this profile is expected to be low. Point 315 m is recommended for drilling.

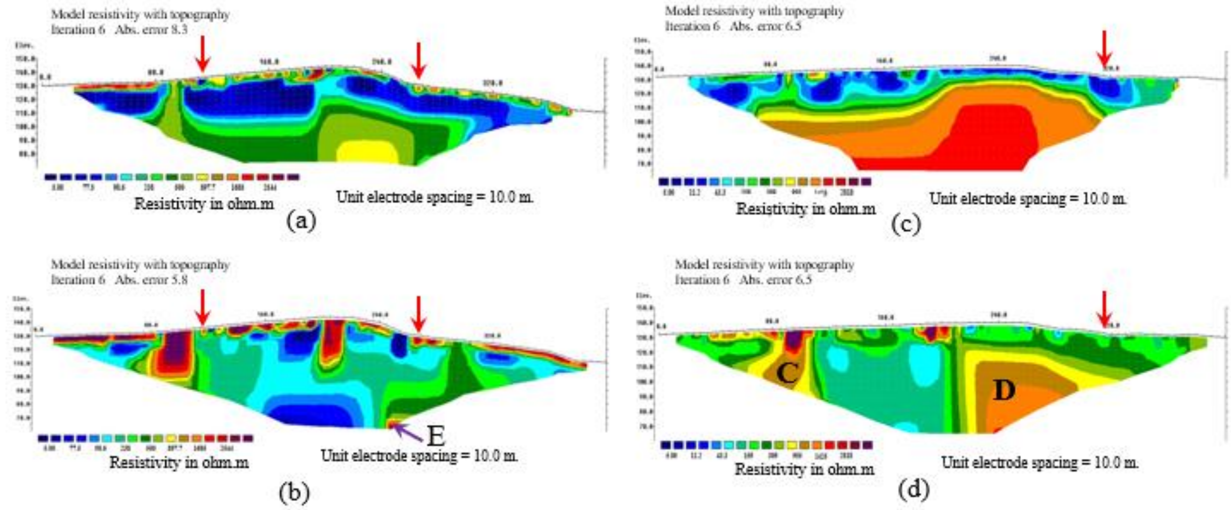

Figure 8: The diagram represents gradient and Wenner resistivity models, where (a) and (b) are for Ahontor and (c) and (d) for Mempeasem communities respectively.

Similarly, results of the Atebubu College of Education and New Amanfrom have revealed potentially competent bedrock blocks (marked A) of resistivity values ranging from 797 to 2114 Ωm for the College of Education and 679 to 2019 Ωm for the New Amanfrom communities at some locations on the profiles. On both measurement techniques at the Atebubu College of Education, rocks of the middle belt are projected to be heavily fractured with possibility of high water contents. The green contours dominating the middle belt have moderate resistivity values ranging from 145 to 243 Ωm (Figures 9 a & b). Locations on the profile that are more likely to intercept the water contents are 135 and 310 m. For the New Amanfrom community expressions of fracturing or faulting were recorded in the middle belt, but with intrusions of clay contents. Structures resolved appear to be better aligned at points 105 and 215 m. In both communities the gradient array results projects confined aquifer systems while the Wenner array results does not. Groundwater potentials for both communities could be moderate to high.

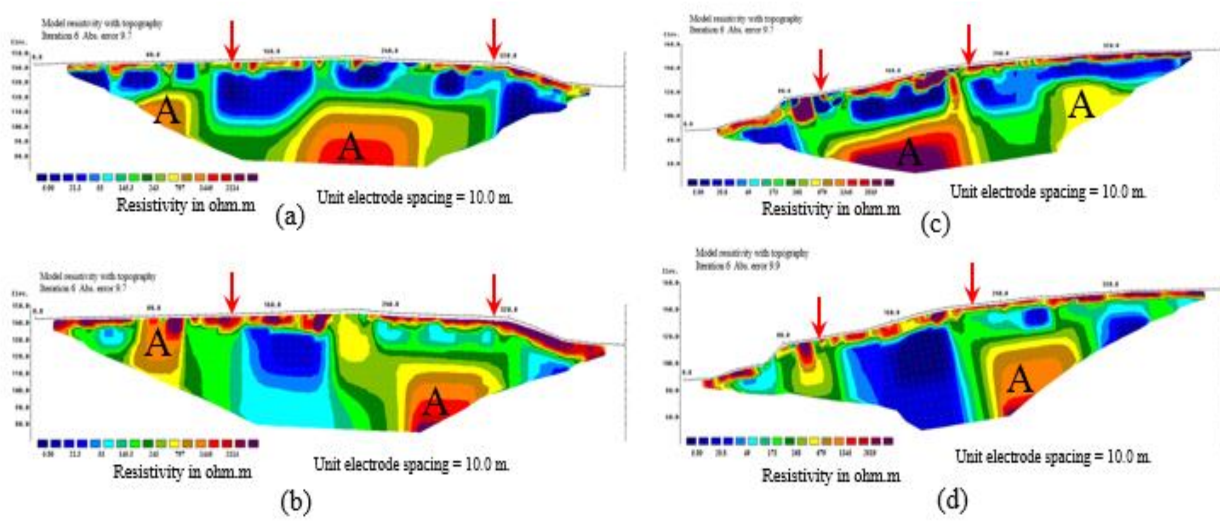

Figure 9: The diagram represents gradient and Wenner resistivity models. (a) and (b) are for Atebubu College of Education and (c) and (d) for New Amanfrom communities respectively.

A plot of all the resistivity data (Figure 10) reveals an interesting subsurface with an admixture of low, moderate and high resistivity distributions. The moderate to high resistivity distributions, indicated by the green contours on this map could be water contents while the high resistivity yellow to deep red contoured layers are interpreted as impervious rock formations (Mainoo et al., 2019; Madun et al., 2018). Clay contents are represented by the low resistivity distributions (indicated by the blue contours). The map projects high groundwater potentials in the middle and north eastern belts. The northern and eastern stretches are characterised by hard rock conditions whose groundwater potential, according to Varade et al. (2018), Basavarajappa et al. (2013) and Maggirwar & Umrikar (2011) are poor, heterogeneous and complex, owing to the fact that they lack primary porosity. Expressions of hard rock conditions were also recorded at few locations in the north western, southern and south western belts. However, considering that these enclaves are also characterised by low (blue contours) to moderate (green contours) resistivity distributions which are expressions of clay and water contents, groundwater potential of these regions could be low to moderately high. The southern belt could be clay dominated as low resistivity distribution was generally observed over it. The southern belt is therefore expected to result in low to moderately high yielding groundwater potential.

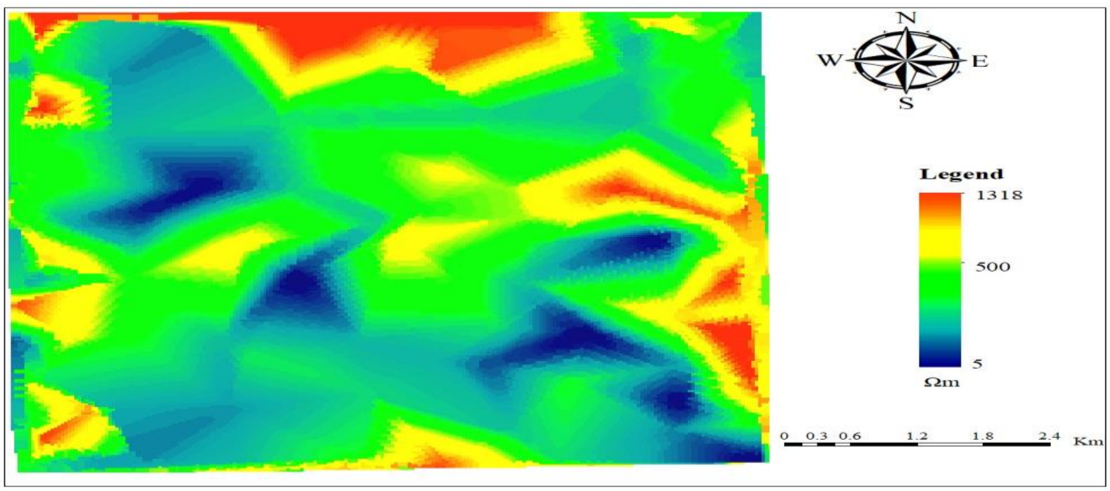

Figure 10: Resistivity model of the study area

5. Depths of existing boreholes in the study area

The various depths of existing boreholes sampled from the Community Water and Sanitation Agency were contoured into different colours (Figure 11) with the red contours being the deepest. Depths in this bracket range from 53.6 to 70.1 m, constituting about 7 % of all the borehole depths sampled. At the time of this survey only few boreholes of this depth bracket were productive. Depths ranges of 39.2 – 40.9 m and 40.9 – 53.6 m constitute about 15 and 20 % respectively while about 28 and 30 % are occupied by depth ranges of 34.5 – 39.2 m and 24.3 – 34.5 m respectively. The map appears to suggest that most boreholes in the municipality are drilled to a maximum depth of 35m, which is too shallow and possibly part of the reasons they dry up in the dry season.

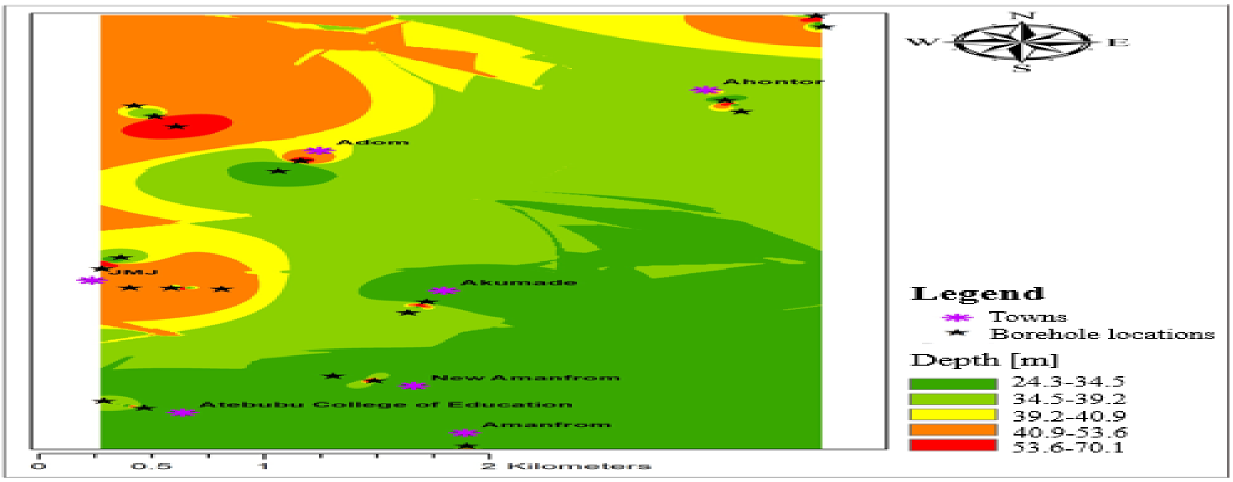

Figure 11: A map showing the depth distribution of existing boreholes in the study area

6. Conclusion

This research was conducted to evaluate the potential of groundwater resources in the Atebubu municipality of Ghana. At the end of the survey, 20 groundwater potential locations expected to be high yielding were identified across the 10 researched communities. Locations identified include the following: 230 and 90 m for Akumade and 190 m for Amanfrom communities. At Akumade, point 230 m was ranked above point 90 m. At the Adom and JMJ School communities, two profiles were investigated. At the end of the survey points 215 and 210 m respectively for profiles 1 and 2 were identified for drilling at Adom. For the JMJ School community points 110 and 195 m were observed to be suitable for drilling on profile 1 while 90 and 260 m were identified for profile 2. Between points 110 and 195 m on profile 1, point 195 m is more preferred. Point 90 m is also preferred to 260 m on profile 2 because of the topography of the area. Points 115 and 265 m were also earmarked for possible drilling at the Ahontor community, where 265 m is expected to be high yielding than 115 m. At Mempeasem only point 315 m was identified as suitable for drilling. Other viable points were sited at points 135 and 310 m at the Atebubu College of Education and 105 and 215 m at the New Amanfrom communities. Of these, points 135 and 215 m respectively are ranked over 310 and 105 m.

In all, the results indicate a clay or shale dominated shallow vadose zone with high probability of a heavily fractured bed rock at deeper depths. Clay easily loses its porosity when wet, therefore allowing water to flow instead of storing it or allowing it to infiltrate into the groundwater system. Hence, the dominance of clay in the shallow subsurface may affect vertical recharge of the aquifer system, especially from rainfall and other surface waters. A lot of the models, especially with the gradient measurements, point to a confined aquifer system. There were also indications of unconfined and perched water contents at few locations on some of the profiles. Across the globe over 1.73 million people die every year from water, sanitation, and hygiene-related diseases such as cholera, diarrhoea, etc. The outcome of this research will inform investors and the government of the plight of communities across the Atebubu municipality since this is the first time such a survey is conducted in the municipality. Borehole drillers and hand-dug well contractors in the municipality use traditional methods of siting aquifers prior to drilling. The outcome of this research will provide them with firsthand information on where to drill or dig high-yielding boreholes or wells.

References

Abonkrah, C. K. (2004). Environmental and Natural Resources Management and Sustainable Rural Development in the Atebubu District, Ghana (Doctoral dissertation, Ohio University).

Acharya, B. S., Halihan, T., Zou, C. B. and Will, R. E. (2017). Vegetation controls on the spatio-temporal heterogeneity of deep moisture in the unsaturated zone: A hydrogeophysical evaluation. Scientific Reports, 7(1), 1499.

Afrose, T., Anthony, L., Fernandez, K. and Latt, S. (2018). Global access to clean water: the role of rain water harvesting. Annals of Reviews and Research, 2, 555585.

Agyare, A., Kabo-Bah, A. T., Bayel, B. T. and Jalloh, A. S. (2021). Integration of GIS and F-Hydra Model for Aquifer Vulnerability Monitoring in the Afram Plains, Ghana. Journal of Geoscience and Environment Protection, 9(03), 222.

Agyekum, W. A. and Asare, E. B. (2016). Challenges associated with ground water resources development in northern Ghana. Ghana Journal of Science, 56(1), 39-51.

Agyekum, W., Klitten, K., Armah, T., Banoeng-Yakubo, B., and Amartey, E. O. (2013). Geophysical borehole logging for control of driller's records: hydrogeological case study from Voltaian sedimentary rocks in northern Ghana. Applied Water Science, 3(2), 491-500.

Akayuli, C., Ofosu, B., Nyako, S. O. and Opuni, K. O. (2013). The influence of observed clay content on shear strength and compressibility of residual sandy soils. International Journal of Engineering Research and Applications (IJERA). Vol. 3, Issue 4, pp. 2538-2542.

Alazard, M., Boisson, A., Maréchal, J. C., Perrin, J., Dewandel, B., Schwarz, T., ... and Ahmed, S. (2016). Investigation of recharge dynamics and flow paths in a fractured crystalline aquifer in semi-arid India using borehole logs: implications for managed aquifer recharge. Hydrogeology journal, 24(1), 35-57.

Almanza Tovar, O. G., Ramos Leal, J. A., Tuxpan Vargas, J., de Jesús Hernández García, G. and De Lara Bashulto, J. (2020). Contrast of aquifer vulnerability and water quality indices between a unconfined aquifer and a deep aquifer in arid zones. Bulletin of Engineering Geology and the Environment, 79, 4579-4593.

Andrews, N. D., Aning, A. A., Danuor, S. K. and Noye, R. M. (2013). Geophysical investigations at the proposed site of the KNUST teaching hospital building using the 2D and 3D resistivity imaging techniques. International Research Journal of Geology and Mining, 3(3), 113-123.

Aning, A. A., Sackey, N., Jakalia, I. S., Sedoawu, O., Tetteh, E. H., Hinson, G., ... and Quaye, E. K. (2014). Electrical resistivity as a geophysical mapping tool; a case study of the new art department, KNUST-Ghana. International Journal of Scientific and Research Publications, 4(1), 1-7.

Appiah-Adjei, E. K. and Osei-Nuamah, I. (2017). Hydrogeological evaluation of geological formations in Ashanti Region, Ghana. Journal of Science and Technology (Ghana), 37(1), 34-50.

Arifin, M. H., Kayode, J. S., Izwan, M. K., Zaid, H. A. H. and Hussin, H. (2019). Data for the potential gold mineralization mapping with the applications of Electrical Resistivity Imaging and Induced Polarization geophysical surveys. Data in brief, 22, 830-835.

Asare-Donkor, N. K. and Adimado, A. A. (2020). Groundwater quality assessment in the Northern and Upper East Regions of Ghana. Environmental Earth Sciences, 79(10), 1-19.

Azizan, F. A., Sah, S. S. and Nawawi, M. M. (2018). Validation of Groundwater Potential Zone Based on Imaging Profiles using Different Array and Lines of Survey Position. In IOP Conference Series: Materials Science and Engineering. IOP Publishing, 429(1), p. 012027.

Banoeng-Yakubu, B., Yidana, S. M., Ajayi, J. O., Loh, Y. & Aseidu, D. (2011). Hydrogeology and groundwater resources of Ghana: a review of the hydrogeology and hydrochemistry of Ghana. Potable Water and Sanitation, 142.

Basavarajappa, H. T., Dinakar, S., Sathish, M. V., Nagesh, D., Balasubramanian, A. and Manjunatha, M. C. (2013). Delineation of groundwater potential zones in hard rock terrain of Kollegal shear zone (Ksz), south India using remote sensing and GIS. International Journal of Earth Sciences and Engineering, 6(5), 1185-1194.

Bienibuor, A. K., Preko, K., Aning, A. A., Antwi, M. and Emahi, I. (2020). Application of Electromagnetic and Electrical Resistivity Methods for Borehole Siting in Low-Grade Metavolcanic and Metasedimentary Rocks, Sunyani West, Ghana. Journal of Environment and Earth Science. 10 (10), 44 - 55.

Bienibuor, A. K., Preko, K., Wemegah, D. D. and Manu, E. (2016). The use of electromagnetic and electrical resistivity methods in assessing groundwater resource potentials in Adoe, Sunyani, Ghana. International Journal of Scientific and Technology Research, 5(9), 166-170.

Cao, G., Scanlon, B. R., Han, D. and Zheng, C. (2016). Impacts of thickening unsaturated zone on groundwater recharge in the North China Plain. Journal of hydrology, 537, 260-270.

Carlson, M. A., Lohse, K. A., McIntosh, J. C. and McLain, J. E. (2011). Impacts of urbanization on groundwater quality and recharge in a semi-arid alluvial basin. Journal of Hydrology, 409(1-2), 196-211.

Chegbeleh, L. P., Akurugu, B. A. and Yidana, S. M. (2020). Assessment of groundwater quality in the Talensi District, Northern Ghana. The Scientific World Journal, 2020; 1-24
Dahlin, T., Leroux, V. and Nissen, J. (2002). Measuring techniques in induced polarisation imaging. Journal of Applied Geophysics, 50(3), 279-298.
Egbueri, J. C. and Mgbenu, C. N. (2020). Chemometric analysis for pollution source identification and human health risk assessment of water resources in Ojoto Province, southeast Nigeria. Applied Water Science, 10(4), 1-18.
Entsua-Mensah, R. M., Essegbey, G., Frempong, G. and Engmann, C. (2007). Assessment of community water and sanitation in Ghana.
Essien, O. E. and Bassey, E. D. (2012). Spatial variation of borehole water quality with depth in Uyo Municipality, Nigeria. In 21st Century Watershed Technology: Improving Water Quality and Environment Conference Proceedings, May 27-June 1, 2012, Bari, Italy (p. 1). American Society of Agricultural and Biological Engineers.
Forkuor, G., Pavelic, P., Asare, E. and Obuobie, E. (2013). Modelling potential areas of groundwater development for agriculture in northern Ghana using GIS/RS. Hydrological sciences journal, 58(2), 437-451.
Fynn, O. F., Yidana, S. M., Chegbeleh, L. P. and Yiran, G. B. (2016). Evaluating groundwater recharge processes using stable isotope signatures—the Nabogo catchment of the White Volta, Ghana. Arabian Journal of Geosciences, 9, 1-15.
Gebere, S. B., Alamirew, T., Merkel, B. J., & Melesse, A. M. (2016). Land use and land cover change impact on groundwater recharge: The Case of Lake Haramaya watershed, Ethiopia. In Landscape Dynamics, Soils and Hydrological Processes in Varied Climates (pp. 93-110). Springer, Cham.
Gemitzi, A., Petalas, C., Tsihrintzis, V. A. and Pisinaras, V. (2006). Assessment of groundwater vulnerability to pollution: a combination of GIS, fuzzy logic and decision-making techniques. Environmental Geology, 49, 653-673.
Ghazavi, R., & Ebrahimi, H. (2018). Predicting the impacts of climate change on groundwater recharge in an arid environment using modeling approach. International Journal of Climate Change Strategies and Management.
Ghestem, M., Sidle, R. C. and Stokes, A. (2011). The influence of plant root systems on subsurface flow: implications for slope stability. Bioscience, 61(11), 869-879.
Gyau-Boakye, P. and Dapaah-Siakwan, S. (2000). Groundwater as source of rural water supply in Ghana. Journal of Applied Science and Technology, 5(1), 77-86.
Hadzi, G. Y., Ayoko, G. A., Essumang, D. K. and Osae, S. K. (2019). Contamination impact and human health risk assessment of heavy metals in surface soils from selected major mining areas in Ghana. Environmental geochemistry and health, 41(6), 2821-2843.
Haidu, I. and Nistor, M. M. (2020). Long-term effect of climate change on groundwater recharge in the Grand Est region of France. Meteorological Applications, 27(1), e1796.
Hakim, M. A., Juraimi, A. S., Begum, M., Hasanuzzaman, M., Uddin, M. K. and Islam, M. M. (2009). Suitability evaluation of groundwater for irrigation, drinking and industrial purposes. American Journal of Environmental Sciences, 5(3), 413-419.
Ho, N. and Sa, N. (2014). Groundwater resources of the Niger Delta: Quality implications and management considerations. International Journal of water resources and environmental engineering, 6(5), 155-163.
Hristopulos, D. T. (2003). Renormalization group methods in subsurface hydrology: overview and applications in hydraulic conductivity upscaling. Advances in Water Resources, 26(12), 1279-1308.
Hussain, Y., Uagoda, R., Borges, W., Nunes, J., Hamza, O., Condori, C., ... and Cárdenas-Soto, M. (2020). The potential use of geophysical methods to identify cavities, sinkholes and pathways for water infiltration. Water, 12(8), 2289.
Juanah, M. S., Ibrahim, S., Sulaiman, W. N. A. and Latif, P. A. (2013). Groundwater resources assessment using integrated geophysical techniques in the southwestern region of Peninsular Malaysia. Arabian Journal of Geosciences, 6(11), 4129-4144.
Li, S., Liu, B., Xu, X., Nie, L., Liu, Z., Song, J., ... and Fan, K. (2017). An overview of ahead geological prospecting in tunneling. Tunnelling and Underground Space Technology, 63, 69-94.
Madun, A., Tajudin, S. A. A., Sahdan, M. Z., Dan, M. F. M. and Talib, M. K. A. (2018). Electrical resistivity and induced polarization techniques for groundwater exploration. International Journal of Integrated Engineering, 10(8).

Maggirwar, B. C. and Umrikar, B. N. (2011). Influence of various factors on the fluctuation of groundwater level in hard rock terrain and its importance in the assessment of groundwater. Journal of Geology and Mining Research, 3(11), 305-317.

Mainoo, P. A., Manu, E., Yidana, S. M., Agyekum, W. A., Stigter, T., Duah, A. A. and Preko, K. (2019). Application of 2D-Electrical resistivity tomography in delineating groundwater potential zones: Case study from the voltaian super group of Ghana. Journal of African Earth Sciences, 160, 103618.

Manley, E., Ogneva-Himmelberger, Y., Ruelle, M., Hanumantha, R., Mazari-Hiriart, M. and Downs, T. J. (2022). Land-cover change and urban growth in the Mexico-Lerma-Cutzamala Hydrological Region, 1993–2018. Applied Geography, 147, 102785.

Margat, J. and Van der Gun, J. (2013). Groundwater around the world: a geographic synopsis. Crc Press. Taylor and Francis Group.

Martínez, J., Rey, J., Sandoval, S., Hidalgo, M. and Mendoza, R. (2019). Geophysical prospecting using ERT and IP techniques to locate Galena veins. Remote Sensing, 11(24), 2923.

Mashhadi, S. R. and Ramazi, H. (2018). The application of resistivity and induced polarization methods in identification of skarn alteration haloes: A case study in the Qale-Alimoradkhan Area. Journal of Environmental and Engineering Geophysics, 23(3), 363-368.

Mashhadi, S. R., Nikfarjam, M. and Mehrnia, A. K. (2020). Reinterpretation of resistivity and induced polarization data to explore gold mineralization zones at Zarzima prospect, Iran. Acta Geol. Slovaca, 12(1), 15-22.

Maxwell, R. M. and Kollet, S. J. (2008). Quantifying the effects of three-dimensional subsurface heterogeneity on Hortonian runoff processes using a coupled numerical, stochastic approach. Advances in water resources, 31(5), 807-817.

Miller, C. R., Routh, P. S., Brosten, T. R. and McNamara, J. P. (2008). Application of time-lapse ERT imaging to watershed characterization. Geophysics, 73(3), G7-G17.

Naeem, U. A., Gabriel, H. F., Khan, N. M., Ahmad, I., Ur Rehman, H. and Zafar, M. A. (2021). Impact of urbanization on groundwater levels in Rawalpindi City, Pakistan. Pure and Applied Geophysics, 178(2), 491-500.

Naik, P. K., Tambe, J. A., Dehury, B. N., & Tiwari, A. N. (2008). Impact of urbanization on the groundwater regime in a fast growing city in central India. Environmental monitoring and assessment, 146(1), 339-373.

Nepf, H., Puijalon, S. and Capra, H. (2022). Organism-scale interaction with hydraulic conditions. Journal of Ecohydraulics, 7(1), 1-3.

Nero, C., Aning, A. A., Danuor, S. K. and Noye, R. M. (2016). Delineation of graves using electrical resistivity tomography. Journal of Applied Geophysics. Vol. 126; pp. 138–147.

Osei, M. A., Amekudzi, L. K., Wemegah, D. D., Preko, K., Gyawu, E. S. and Obiri-Danso, K. (2017). Hydro-Climatic Modelling of an Ungauged Basin in Kumasi, Ghana. Hydrology and Earth System Sciences Discussions, 1-19.

Owuor, S. O., Butterbach-Bahl, K., Guzha, A. C., Rufino, M. C., Pelster, D. E., Díaz-Pinés, E. and Breuer, L. (2016). Groundwater recharge rates and surface runoff response to land use and land cover changes in semi-arid environments. Ecological Processes, 5(1), 1-21.

Pellicer, X. M. and Gibson, P. (2011). Electrical resistivity and Ground Penetrating Radar for the characterisation of the internal architecture of Quaternary sediments in the Midlands of Ireland. Journal of Applied Geophysics, 75(4), 638-647.

Praamsma, T., Novakowski, K., Kyser, K. and Hall, K. (2009). Using stable isotopes and hydraulic head data to investigate groundwater recharge and discharge in a fractured rock aquifer. Journal of Hydrology, 366(1-4), 35-45.

Preko, K., Scheuermann, A. and Wilhelm, H. (2009). Comparison of invasive and non-invasive electromagnetic methods in soil water content estimation of a dike model. Journal of Geophysics and Engineering, 6(2), 146-161.

Razak, M. H. and Muztaza, N. M. (2022). Evaluation of aquifer potential using 2-D resistivity and induced polarization in Machang, Kelantan, Malaysia. Journal of Sustainability Science and Management, 17(1), 259-270

Rucker, D. F., Noonan, G. E. and Greenwood, W. J. (2011). Electrical resistivity in support of geological mapping along the Panama Canal. Engineering Geology, 117(1-2), 121-133.

Saha, D., Marwaha, S. and Mukherjee, A. (2018). Groundwater resources and sustainable management issues in India. Clean and sustainable groundwater in India, 1-11.

Sasidharan, S., Bradford, S. A., Šimůnek, J. and Kraemer, S. R. (2020). Groundwater recharge from drywells under constant head conditions. Journal of hydrology, 583, 124569.

Scanlon, B. R., Reedy, R. C., Stonestrom, D. A., Prudic, D. E. and Dennehy, K. F. (2005). Impact of land use and land cover change on groundwater recharge and quality in the southwestern US. Global Change Biology, 11(10), 1577-1593.

Shahbazi, A., Saeidi, A. and Chesnaux, R. (2020). A review of existing methods used to evaluate the hydraulic conductivity of a fractured rock mass. Engineering Geology, 265, 105438.

Sharp, J. M. (2010). The impacts of urbanization on groundwater systems and recharge. AQUA mundi, 1(3).

Smerdon, B. D., Mendoza, C. A. and Devito, K. J. (2008). Influence of subhumid climate and water table depth on groundwater recharge in shallow outwash aquifers. Water Resources Research, 44(8).

Sowley, E. N. K. and Aboagye, E. (2010). Constraints to vegetable seed procurement and production in the Atebubu-Amantin District of Brong-Ahafo region of Ghana. Ghana Journal of Horticulture, 8, 85-91.

Stober, I. and Bucher, K. (2015). Hydraulic conductivity of fractured upper crust: insights from hydraulic tests in boreholes and fluid-rock interaction in crystalline basement rocks. Geofluids, 15(1-2), 161-178.

Sunkari, E. D., Abu, M. and Zango, M. S. (2021). Geochemical evolution and tracing of groundwater salinization using different ionic ratios, multivariate statistical and geochemical modeling approaches in a typical semi-arid basin. Journal of Contaminant Hydrology, 236, 103742.

Tahiru, A. A., Doke, D. A. and Baatuuwie, B. N. (2020). Effect of land use and land cover changes on water quality in the Nawuni Catchment of the White Volta Basin, Northern Region, Ghana. Applied Water Science, 10(8), 1-14.

Taylor, R. G., Scanlon, B., Döll, P., Rodell, M., Van Beek, R., Wada, Y., ... and Treidel, H. (2013). Ground water and climate change. Nature climate change, 3(4), 322-329.

Togbévi, Q. F., Van Der Ploeg, M., Tohoun, K. A., Agodzo, S. K. and Preko, K. (2022). Assessing the Effects of Anthropogenic Land Use on Soil Infiltration Rate in a Tropical West African Watershed (Ouriyori, Benin). Applied and Environmental Soil Science, 2022.

Varade, A. M., Khare, Y. D., Yadav, P., Doad, A. P., Das, S., Kanetkar, M. and Golekar, R. B. (2018). 'Lineaments' the potential groundwater zones in hard rock area: a case study of basaltic terrain of WGKKC-2 watershed from Kalmeswar Tehsil of Nagpur District, Central India. Journal of the Indian Society of Remote Sensing, 46, 539-549.

Wakode, H. B., Baier, K., Jha, R. and Azzam, R. (2018). Impact of urbanization on groundwater recharge and urban water balance for the city of Hyderabad, India. International Soil and Water Conservation Research, 6(1), 51-62.

Yesilnacar, M. I. and Sahinkaya, E. (2012). Artificial neural network prediction of sulfate and SAR in an unconfined aquifer in southeastern Turkey. Environmental Earth Sciences, 67, 1111-1119.

Yidana, S. M. and Yidana, A. (2010). An assessment of the origin and variation of groundwater salinity in southeastern Ghana. Environmental Earth Sciences, 61(6), 1259-1273.

Yidana, S. M., Ophori, D. and Banoeng-Yakubo, B. (2008). Hydrogeological and hydrochemical characterization of the Voltaian Basin: the Afram Plains area, Ghana. Environmental Geology, 53(6), 1213-1223.

Yidana, S. M., Ophori, D. and Alo, C. A. (2014). Hydrogeological characterization of a tropical crystalline aquifer system. Journal of Applied Water Engineering and Research, 2(1), 13-24.

Yidana, S. M., Vakpo, E. K., Sakyi, P. A., Chegbeleh, L. P. and Akabzaa, T. M. (2019). Groundwater–lakewater interactions: an evaluation of the impacts of climate change and increased abstractions on groundwater contribution to the Volta Lake, Ghana. Environmental Earth Sciences, 78(3), 1-16.

Yifru, B. A., Chung, I. M., Kim, M. G. and Chang, S. W. (2021). Assessing the effect of land/use land cover and climate change on water yield and groundwater recharge in East African Rift Valley using integrated model. Journal of Hydrology: Regional Studies, 37, 100926.

Zhang, H., Shi, Z., Wang, G., Sun, X., Yan, R. and Liu, C. (2019). Large earthquake reshapes the groundwater flow system: Insight from the water-level response to earth tides and atmospheric pressure in a deep well. Water Resources Research, 55(5), 4207-4219.

Zhu, K., Bayer, P., Grathwohl, P. and Blum, P. (2015). Groundwater temperature evolution in the subsurface urban heat island of Cologne, Germany. Hydrological processes, 29(6), 965-978.

Zomlot, Z., Verbeiren, B., Huysmans, M. and Batelaan, O. (2017). Trajectory analysis of land use and land cover maps to improve spatial–temporal patterns, and impact assessment on groundwater recharge. Journal of Hydrology, 554, 558-569.